Magnetization studies of $(GeTe)_{1-x}(MnTe)_x$ pseudobinary alloys

R. W. Cochrane, M. Plischke*, and J. O. Ström-Olsen
Eaton Research Laboratory, McGill University, Montreal 101, Quebec, Canada
(Received 17 October 1973)

We present measurements and analysis of the magnetic properties of the degenerate magnetic semiconductor $(GeTe)_{1-x}(MnTe)_x$ for $0<x<0.5$. The measurements were made in fields of up to 55 kOe over the temperature range 1–350 °K. The results fall into two parts. For $x<0.15$, the properties are well explained by a simple Ruderman-Kittel-Kasuya-Yosida (RKKY) theory with an exchange constant between the manganese and the free carriers of 0.9 ± 0.09 eV, in excellent agreement with a previously reported independent determination from transport properties. For $x>0.20$, the experimental results deviate strongly from the predictions of this simple model and exhibit some striking properties which we believe to be intrinsic. Suggestions are offered for the causes of these deviations.

I. INTRODUCTION

The pseudobinary alloy $(GeTe)_{1-x}(MnTe)_x$ provides an excellent system for studying the interactions between magnetic ions diluted in an electron gas of low metallic density. MnTe and GeTe are structurally quite similar and the two may be alloyed over a wide range of concentration[1] with the result that the distance between the magnetic ions may also be varied over a wide range. Furthermore, the system is a degenerate semiconductor containing about 10^{21} carriers/cm^3 so that the density of the conduction-electron gas is intermediate between that of a metal and that of a nondegenerate semiconductor.

The first magnetic studies were carried out by Rodot *et al.*[2] who reported that the system orders ferromagnetically even though MnTe itself is antiferromagnetic.[3] However, they were unable to provide a consistent description of the system or to make quantitative deductions. More recently, two of the present authors[4] presented measurements on alloys containing low concentrations of MnTe and found ferromagnetic ordering with a paramagnetic Curie-Weiss temperature which varied linearly with concentration at the rate 4.4 °K per at.% MnTe. This behavior[2] was interpreted on the basis of a Rudermann-Kittel-Kasuya-Yosida (RKKY) interaction characterized by an exchange interaction between the conduction electrons and the manganese ions with an exchange constant J_{sd}. Later, measurements of magnetoresistivity were made[5] on a sample containing 1-at.% MnTe. The results were very well explained by the above model with a value for J_{sd} of 0.8 ± 0.08 eV.

In the present paper, we have extended the range of MnTe concentration to 50 at.% and have made a more exhaustive study of the magnetic properties, including an investigation of the spin dynamics through the temperature dependence of the magnetization below the ordering temperature. It is found that for samples containing up to 15-at.% MnTe, the magnetic data are accurately described by the RKKY model, yielding a value for J_{s-d} in excellent agreement with the independent determination from transport measurements mentioned above. The behavior of samples containing over 15-at.% MnTe, however, is very poorly described, particularly with regard to the temperature dependence of the magnetization. At the present time no quantitative explanation exists for these anamolies, but a number of possible causes are suggested.

In this paper, the sample preparation and measurement techniques are described in Sec. II, followed by the experimental results in Sec. III. These data are suggestive of a long-range indirect exchange model of the RKKY type which is outlined in Sec. IV for a random substitutional alloy. In Sec. V, the theory and experimental results are compared and the paper is concluded in Sec. VI.

II. SAMPLE PREPARATION AND MEASUREMENT TECHNIQUES

A. Sample preparation

The phase diagram[1] for the $(GeTe)_{1-x}(MnTe)_x$ system exhibits three stable solid phases at room temperature which become one phase at high temperatures just below the solidus curve. The high-temperature phase is the simple cubic NaCl structure common to a large number of chalcogenide compounds. Below 450 °C, however, the stable phase for GeTe is a distorted cubic structure with a corner angle of 88°. For low concentrations of MnTe, the stable phase is also a distorted cubic, but the corner angle increases continuously with MnTe reaching 90° at about 18 at.%. From 18 to 60 at.% the phase is the high-temperature cubic NaCl. The lattice parameter also varies smoothly with MnTe, going from 5.98 Å in pure GeTe to 5.88 Å in the 60-at.% alloy. Beyond 90 at.%, the alloys crystallize into the hexagonal NiAs structure of MnTe, while the region between 60 and 90 at.% is two-phase.

All the alloys were made starting from high-purity elements, all of 99.999% purity. Pure GeTe

was made by reacting the elements together in a sealed and evacuated ($\leq 10^{-4}$ Torr) quartz ampoule at 800 °C for 3 h. Pure MnTe was made by dissolving Mn powder in molten Te in a graphite crucible under vacuum at 900 °C for 24 h. X-ray powder photographs confirmed that both compounds had the expected crystal structure. The pseudobinary alloys $(GeTe)_{1-x}(MnTe)_x$ were then made by mixing GeTe and MnTe in the desired proportions in an evacuated sealed quartz ampoule and heating first for 6–12h above the solidus temperature (800–850 °C), and then annealing below it (720–750 °C) for 24–48 h. The latter procedure proved especially important for ensuring uniformity in the higher-concentration alloys. One sample (30 at.%) was also annealed at 720 °C for a further 2 weeks, but there was no detectable change after this anneal, either in structural or in magnetic properties.

An electron-microprobe analysis of the annealed specimens revealed MnTe concentrations x close to the starting proportions as well as a uniform distribution ($\sim 0.1x$) over the size of the beam (1 $\mu\nu$). Table I shows a list of the samples with the nominal and actual concentrations as determined from the microprobe, the latter being used as the sample concentrations for subsequent calculations.

B. Apparatus

The mobile-carrier densities were deduced from a measurement of the Hall voltage using the circuit described in an earlier paper.[5] The carrier numbers, also listed in Table I, were found to be independent of temperature and to increase only gradually with MnTe concentration, at least as far as 25 at.%. For the three highest concentrations we were unable to produce samples suitable for the Hall-effect measurements and consequently the carrier density for these alloys is unknown.

The magnetization was measured by means of a vibrating sample magnetometer (VSM) designed to operate in the axial field of a 60-kOe NbTi superconducting solenoid. A pair of pickup coils were wound in series opposition on a phenolic former which was mounted rigidly in the magnet bore, as described by Olivera and Foner.[6] Over-all sensitivity of this system is approximately $(1-3)\times 10^{-4}$ emu.

The sample holder was a fiberglass rod, approximately 3 cm long and 0.6 cm in diameter, with one end drilled out as a sample chamber. The fiberglass rod also served both as a mount for a GaAs-diode thermometer and as a former for a small copper reference coil wound around the sample chamber. In operation, the pickup coils were used as null detectors in a feedback loop which controlled the current in the reference coil so as to balance the signal generated by the samples. Hence, the feedback current to the reference coil provides a continuous and direct measure of the magnetic moment of the sample independent of vibration amplitude and sample position. Furthermore, this technique eliminates, at least to first order, the field-dependent image effects[7] in the superconducting magnet, since the combined system of sample and reference coil has no net magnetic moment. A similar apparatus has recently been described by Springford *et al.*[8]

The sample temperature could be varied over the range from 1.1 to 300 °K by isolating the sample in a separate insert Dewar. Below 4.2 °K the temperature was controlled by regulating the vapor pressure of liquid helium and read directly from the vapor-pressure tables. Above 4.2 °K, a GaAs diode (Lakeshore Cryotronics, Inc., TG 100 P/M) calibrated to 0.1 °K was used both for measuring and controlling the sample temperature. The diode voltage was fed to a differential voltmeter whose off-balance voltage was square rooted,

TABLE I. Concentrations of the specimens obtained from microprobe analysis and room-temperature susceptibility together with their carrier density and resistivity.

x (nominal)	x (microprobe)	x (susceptibility)	(10^{+21} holes cm^{-3})	(10^{-4} Ω cm)
Pure GeTe	• • •	• • •	0.92	1.9±0.2
0.002	• • •	0.0025	1.0	1.8±0.2
0.005	0.005±0.002[a]	0.0047	1.1±0.1	1.4±0.2
0.01	0.010±0.002[a]	0.0095	1.15±0.1	2.3±0.2
0.02	0.020±0.005	0.0166	1.2±0.1	2.0±0.2
0.05	0.05±0.005	0.040	1.2±0.1	• • •
0.10	0.09±0.005	0.085	1.5±0.2	• • •
0.15	0.14±0.01	• • •	1.2±0.2	• • •
0.20	0.19±0.01	• • •	2.0±0.2	• • •
0.25	0.21±0.02	• • •	2.0±0.2	• • •
0.30	0.27±0.02	• • •	• • •	• • •
0.40[b]	0.38±0.08	• • •	• • •	• • •
0.50	0.52±0.02	• • •	• • •	• • •

[a]Microprobe resolution was 0.002.

[b]Specimen not heat treated (see text).

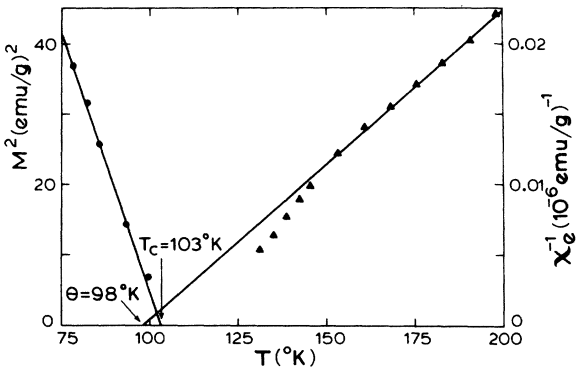

FIG. 1. Temperature dependence of the inverse low-field susceptibility, χ_e^{-1}, above T_C and the square of the magnetization M^2, at $H = 0.5$ kOe below T_C indicating the independent determination of the Curie-Weiss temperature Θ and the ferromagnetic transition temperature T_C.

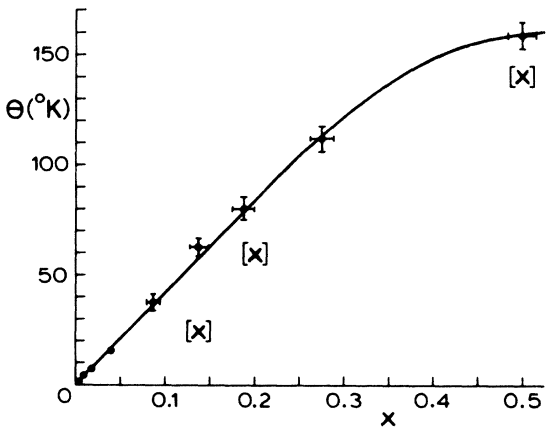

FIG. 2. Curie-Weiss temperature Θ as a function of MnTe concentration x.

amplified, and fed to a unipolarity power supply and resistance heater. With this system, temperature stability was better than ±0.03 °K over the entire temperature range.

III. EXPERIMENTAL RESULTS

We have measured the magnetization of all the samples as a function of the magnetic field from 1.1 °K to room temperature. The data clearly indicate a *ferromagnetic ordering* above 1.1 °K for all the alloys except the one with only 0.2-at.% MnTe. The results are presented separately for the two temperature regimes, $T > T_C$ and $T \leq T_C$.

A. High-temperature data, $T > T_C$

In the paramagnetic regime, the magnetic susceptibility follows a Curie-Weiss relation well above the ordering temperature. The paramagnetic Curie Weiss temperature Θ was determined by plotting the inverse low-field susceptibility, χ_e^{-1} against the temperature T, where the subscript e indicates that the diamagnetic susceptibility of the GeTe host has been subtracted. A number of these graphs for the lower concentrations have been shown in Ref. 6. Figure 1 shows a similar plot for $x = 0.2$. Close to T_C, the more concentrated alloys show deviations from the Curie-Weiss behavior, perhaps the result of a nonuniform distribution of MnTe. The values of Θ and the Curie constant C have been tabulated in Table II for all the samples. Figure 2 shows the concentration dependence of Θ. The crosses represent points obtained from samples *before* the annealing process. These samples revealed considerable nonuniformities of MnTe distribution under the microprobe and the results from them have only been included to emphasize the need for the annealing process.

TABLE II. Values of the Curie-Weiss temperature, Θ; the Curie constant, C; the effective spin of the manganese ion, S_{eff}; ferromagnetic ordering temperature, T_C; extrapolated zero-field magnetic moment, $M(H \to 0)$, at the specified temperature, and the high-field susceptibility X_{hf} at the same temperature.

x (nominal)	Θ(°K)	$C(10^4$ emu/S)	S_{eff}	T_C(°K)	T_C/Θ	$M(0)$emu/g (at T in °K)	$X_{hf}(10^6$ emu/g)
0.002	0.5±0.1	0.8	3.2	• • •	• • •	• • •	• • •
0.005	1.7±0.2	1.22	2.8	• • •	• • •	0.74 (1.1°K)	• • •
0.01	3.3±0.2	2.28	2.7	2.3±0.2	0.7±0.1	1.2 (1.1°K)	1.2
0.02	6.9±0.5	3.65	2.4	6.0±1.0	0.8±0.15	1.69 (4.8°K)	4.5
0.05	18±2	8.8	2.3	9±2	0.5±0.2	3.22 (1.1°K)	15.4
0.10	44±5	13.9	2.2	25±4	0.6±0.2	5.5 (1.1°K)	29.8
0.15	60±5	23.3	2.3	• • •	• • •	8.25 (4.2°K)	• • •
0.20	98±5	45.2	2.8	103±10	1.0±0.15	18.8 (4.2°K)	44.8
0.25	100±5	• • •	• • •	100±10	1.0±0.15	• • •	• • •
0.30	140±10	38.5	2.1	148±4	1.0±0.15	• • •	• • •
0.40[a]	95±8	20.9	1.1	102	1.1±0.2	• • •	• • •
0.50	156±10	57.8	1.8	167	1.1±0.2	• • •	• • •

[a]Not heat treated.

B. Low-temperature data, $T \leq T_C$

The ordering temperatures T_C have been determined independently of the paramagnetic Curie-Weiss temperature using data in the ordered region. In the molecular-field approximation, M^2 is linear in T at low fields. T_C was thus obtained by extrapolating the steep linear part of the M^2-vs-T plot to its temperature intercept as illustrated for the 20-at.% sample in Fig. 1. Below 4.2 °K it was more convenient to measure M as a function of H at constant temperature. Consequently, for the lower MnTe concentrations, T_C was deduced using the usual thermodynamic relation for second-order phase transitions[9]

$$a(T - T_C)M + bM^2 = H ,$$

i.e., a plot of M^2 vs H/M passes through the origin at $T = T_C$. The T_C results for all concentrations are also listed in Table II. It is interesting to note that for all the alloys investigated neither of the characteristic temperatures, Θ or T_C, exceeded 170 °K, a fact which is consistent with Fig. 2 and also the earlier data of Rodot *et al.*[2]

At temperatures well below T_C, the high-field magnetization curves all show several characteristics which are evident in Fig. 3 for $x = 0.5$. The low-field behavior exhibits moderate hysteresis and the maximum coercive field observed was less than 200 Oe at 4.2 °K. Nevertheless, all the samples display a significant high-field susceptibility, χ_{hf}, even at 55 kOe. χ_{hf} was essentially independent of the size or shape of the sample; it was identical for powdered and cast specimens of various lengths and diameters. Evidently, it is an intrinsic property of these alloys. Table II includes χ_{hf} measured at either 1.1 or 4.2 °K, along with the extrapolated $H = 0$ magnetization at the same temperature.

In order to investigate the dynamic character of the magnetic interactions, we have examined in detail the temperature dependence of the magnetization at constant applied magnetic fields sufficient to produce technical saturation ($\geq$ 5 kOe, Fig. 3). The four lowest concentrations were eliminated because their low ordering temperatures made the region $T \ll T_C$ inaccessible to our equipment. Furthermore, small irreproducible background signals from the addenda limited to 25 kOe the applied fields for these precision measurements. Figure 4 presents the $m = M(T)/M(0)$ data as a function of temperature for $x = 0.2$ at 5 kOe through the ordering temperature T_C. The excitation of spin waves predicts that, at temperatures well below T_C, the magnetization should vary as $T^{3/2}G(H, T)$, where $G(H, T)$ is the field and temperature-dependent gap function, as discussed in Sec. IV. This prediction is well followed for the 10-at.% alloy ($x = 0.10$) as is illustrated in Fig. 5. This figure clearly indicates that the low-temperature deviations from simple $T^{3/2}$ behavior is well described by including the gap function. Similar results were also found for $x = 0.05$ and 0.15.

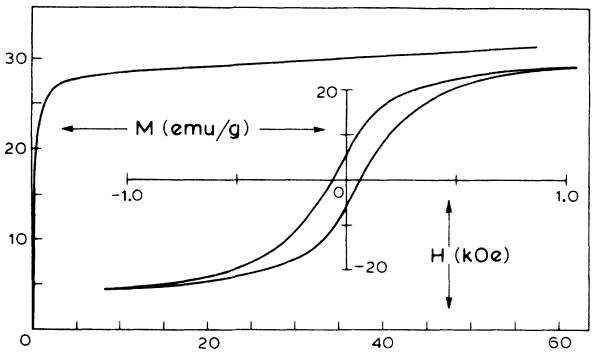

FIG. 3. High-field-magnetization curve for $x = 0.5$ at $T = 4.2$ °K. Insert is a blowup of the low-field region showing the hysteresis and remanence of this sample.

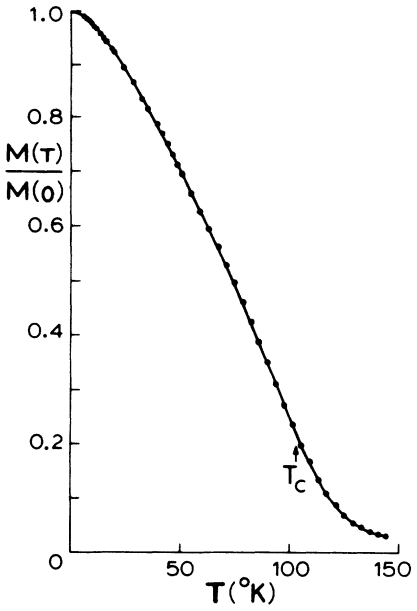

FIG. 4. Reduced magnetization $M(T)/M(0)$, as a function of temperature for the $x = 0.20$ alloy.

Beyond $x = 0.15$, the magnetization-vs-temperature relation is fundamentally different from that of the lower concentration materials. At 20-at.% MnTe the $m(T)$ varies as $T^{3/2}$, a relation which, remarkably, is *field independent*. Beyond $x = 0.2$ the $m(T)$ varies as T^2 and, again, is field independent. In Fig. 6 we have plotted m vs T^2 for 50-at.% MnTe. Figure 7 compares the magnetization curves for $x = 0.05$ and 0.20 at two different temperatures. The curves for the higher concentrations run parallel, a direct illustration of the field independence of $m(T)$. This contrasts the expected

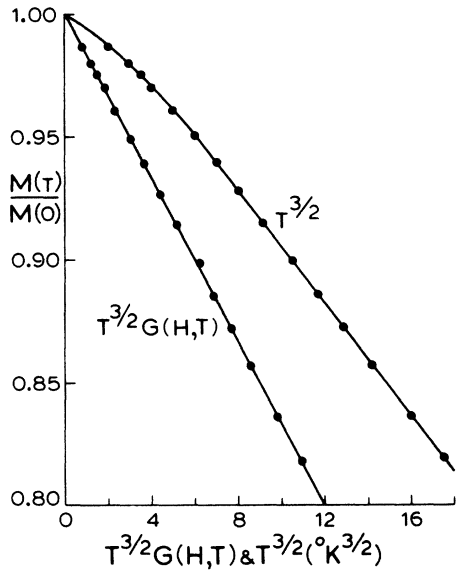

FIG. 5. Reduced magnetization $M(T)/M(0)$ as a function of $T^{3/2}$ and $T^{3/2}$ $G(H,T)$ for the $x=0.10$ alloy.

behavior at the low concentration for which the magnetization curves at different temperatures converge at high fields.

IV. THEORY

Since the alloys under discussion were ferromagnetic even at very low concentrations of manganese, the interaction between the magnetic ions is clearly long range, which suggests that it is of the RKKY type proceeding via the mobile carriers, here holes. The RKKY interaction[10] has been successfully used to describe magnetic behavior of the rare-earth metals and their alloys.[11] Since we are dealing with $3d$ electrons, one might expect that a combination of the localized and band models might be appropriate for this system. Such a model has been proposed by Arai and Parinello[12] and discussed in some detail by Bartel.[13] In this system, however, the manganese atoms seem to have a well defined local moment and we assume the simple RKKY interaction as well as a nearest-neighbor antiferromagnetic (AFM) exchange between the manganese ions, since pure MnTe is AFM. In this section we present a random-phase treatment[14] of this model and in Sec. V compare its predictions with the results already presented.

We therefore write the Hamiltonian for the manganese spins as

$$H = -\frac{1}{2}\sum_{i,j} J(i,j)\vec{S}_i \cdot \vec{S}_j$$

$$= -\frac{1}{2}\sum_{i,j} [J_1(i,j)+J_2(i,j)]\vec{S}_i \cdot \vec{S}_j \,, \qquad (1)$$

where i, j are restricted to sites occupied by the manganese which enter substitutionally for Ge. $J_1(i,j)$ is the usual[10] RKKY interaction:

$$J_1(i,j) = \frac{m^* a_0^2}{64\pi^3\hbar^2} J_{sd}^2 \times \left(\frac{\sin\alpha R_{ij} - \alpha R_{ij}\cos\alpha R_{ij}}{(R_{ij})^4}\right) e^{-R_{ij}/\lambda} \,, \qquad (2)$$

where $\alpha = 2k_f a_0$, k_f being the Fermi momentum of the conduction holes and a_0 the distance between nearest-neighbor Ge or Mn sites. λ is the mean free path of the carriers, R_{ij} is the distance between sites i and j measured in terms of a_0, and J_{sd} is the exchange interaction constant between the conduction holes and the manganese ions. The AFM term, $J_2(i,j)$, is taken as $J_2(<0)$ when i and j are nearest neighbors and zero otherwise. We shall treat J_{sd} and J_2 as variable parameters to be determined from experimental data.

The Hamiltonian is treated by the random-phase approximation[14] (RPA) for spins of general size. We first define the Zubarev[15] Green's function

$$G_{ij}(t,t') = -i\theta(t-t')\langle[S_i^+(t), S_j^-(t')]\rangle \,. \qquad (3)$$

Taking the Fourier transform and using RPA yields the equation of motion

$$\omega G_{ij}(\omega) = \frac{\delta_{ij}}{2\pi}\langle S_i^z\rangle + \sum_l J(i,l) \times \{\langle S_i^z\rangle G_{ij} - \langle S_i^z\rangle G_{lj}\} \,. \qquad (4)$$

In Eq. (4), of course, all indices are restricted to sites occupied by manganese atoms. This restric-

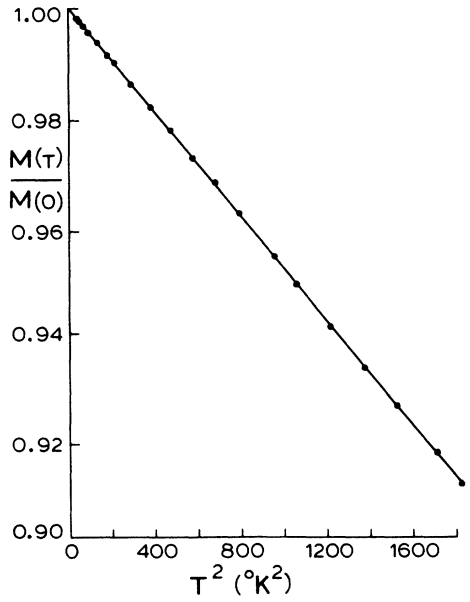

FIG. 6. Reduced magnetization $M(T)/M(0)$ as a function of T^2 for $x=0.50$ alloy.

tion is more conveniently handled by introducing the random variable P_i which is unity when site i is occupied by manganese and zero when not. We then introduce the modified Green's function, G_{ij},

$$G_{ij}(\omega) = P_i P_j G'_{ij}(\omega) \ . \tag{5}$$

So that Eq. (4) becomes

$$\omega P_i P_j G'_{ij}(\omega) = \frac{P_i \delta_{ij} \langle S_i^x \rangle}{2\pi} + \sum_l P_i P_j P_l J(i,l) \{ \langle S_l^x \rangle G'_{ij} - \langle S_i^x \rangle G'_{lj} \} \ . \tag{6}$$

We now assume that G'_{ij} is independent of configuration and average Eq. (6) over all lattice configurations. Assuming uniform distribution of the manganese we have

$$P_i P_j = x(1-x)\delta_{ij} + x^2$$

and, if we neglect the possibility $l = j$ on the right-hand side of equation (6), $\langle P_i P_j P_l \rangle = x \langle P_i P_j \rangle$, where x is the MnTe concentration. Dividing both sides by $\langle P_i P_j \rangle$ makes Eq. (6) translationally invariant with $\langle S_i^x \rangle = \langle S^x \rangle$. Making the transformation

$$G'_{ij} = \frac{1}{N} \sum_q G'(q) e^{i \vec{q} \cdot \vec{R}_{ij}} \tag{7}$$

immediately yields

$$G'(k) = \frac{1}{2\pi} \frac{\langle S^x \rangle}{\omega - x \langle S^x \rangle \{ J(0) - J(k) \}} \ , \tag{8}$$

where

$$J(k) = \sum_{R_{ij}} J(\vec{R}_{ij}) e^{-i \vec{k} \cdot \vec{R}_{ij}} \ .$$

One can show[16] that the expectation value $\langle S^x \rangle$ is obtained from the Green's function via the relation

$$\langle S^x \rangle = \frac{(S - \phi_0)(1+\phi_0)^{2S+1} + (S+1+\phi_0)\phi_0^{2S+1}}{(1+\phi_0)^{2S+1} - \phi_0^{2S+1}} \ , \tag{9}$$

where

$$\phi_0 = \frac{1}{N} \sum_k \left[\exp \{ \beta x \langle S^x \rangle \times [J(0) - J(k)] \} - 1 \right]^{-1} \ . \tag{10}$$

Using these equations one obtains an expression for the ferromagnetic transition temperature

$$T_c = x \frac{S(S+1)}{3k_B} \left(\frac{1}{N} \sum_k \frac{1}{J(0) - J(k)} \right)^{-1} \ , \tag{11}$$

and the paramagnetic Curie-Weiss temperature

$$\Theta = \frac{S(S+1)}{3k_B} x J(0) \ . \tag{12}$$

We note that both these expressions are linear in concentration, as is observed experimentally for the range $0 < x < 0.3$. At this stage we could take the value of J_2 as given by pure MnTe and deduce

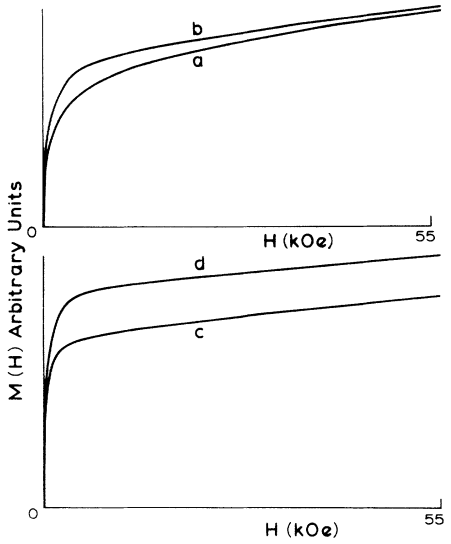

FIG. 7. Magnetization curves at constant temperature for the $x = 0.05$ and 0.20 alloys: upper curves $x = 0.05$ (a) $T = 4.2$ °K, (b) $T = 1.06$ °K; lower curves $x = 0.20$ (c) $T = 6.5$ °K, (d) $T = 39$ °K.

J_{sd} from the slope of Θ vs x as given in Fig. 2. Instead, we calculate the spin-wave spectrum, $\epsilon(k)$, which determines the temperature dependence of the bulk magnetization, $M = xN\langle S_z \rangle$, well below the ordering temperature. The concentration dependence of both the Curie-Weiss Θ and the spin-wave demagnetization is then sufficient to determine J_{sd} and J_2 independently. We first calculate the directionally averaged spin-wave spectrum in the absence of a magnetic field,

$$\epsilon(k) = \frac{1}{4\pi} \int d\Omega_k \epsilon(\vec{k}) = x \langle S^x \rangle \sum_R J(R) \left(1 - \frac{\sin kR}{kR} \right) .$$

We further approximate this function by explicitly *summing* over nearest neighbors and then *integrating* over the rest of the lattice. Since the magnetic atoms occupy an fcc sublattice in the NaCl structure we obtain

$$\epsilon(k) = 12x \langle S^x \rangle \{ J_1(a_0) - J_2 \} \left(1 - \frac{\sin k}{k} \right) + \sqrt{2} x \langle S^x \rangle \int_{r>1} d^3r \, J_1(r) \left(1 - \frac{\sin kr}{kr} \right) . \tag{13}$$

In the presence of an applied magnetic field H the Zeeman energy of each excitation must be added to Eq. (13). Since each spin-wave carries one Bohr magneton, this is simply $g\mu_B H$. To obtain the bulk magnetization M as a function of temperature, Eqs. (9), (10), and (13) must be solved self-consistently. At low temperatures one finds

$$\langle S^z\rangle = S\{1 - AT^{3/2}G(T,H)\}\ , \tag{14}$$

where

$$A = \frac{\zeta(\frac{3}{2})}{4S}\left\{\frac{k_B}{2\pi xD}\right\}^{3/2}\ . \tag{15}$$

ζ is the Riemann Zeta function, and

$$\frac{xD}{k_B}k^2 = \left(\frac{2Sx}{k_B}[J_1(a_0) - J_2] + \frac{2\pi\sqrt{2}}{3k_B}J_1Sx \times \int_1^\infty dy(\sin\alpha y - \alpha y\cos\alpha y)e^{-y/\lambda}\right)k^2 \tag{16}$$

is the leading term in the dispersion relation $\epsilon(k)$ [Eq. (13)] and

$$G(T,H) = \frac{1}{\zeta(\frac{3}{2})}\sum_{x=1}^{\infty} n^{-3/2}e^{-n g\mu_B H/k_B T} \simeq 1 - 1.36\left(\frac{g\mu_B H}{k_B T}\right)^{1/2} + 0.56\frac{g\mu_B H}{k_B T} + \cdots \tag{17}$$

is the gap function.[17]

In summary, this theory predicts a Curie-Weiss temperature linearly dependent upon x and a bulk magnetization whose low-temperature behavior is dominated by spin-wave excitations leading to a demagnetization coefficient which scales as $x^{-3/2}$.

V. COMPARISON WITH EXPERIMENT

The data presented in Sec. III show a clear change in character between 15- and 20-at.% MnTe, dividing the alloys into two groups—low concentrations and high concentrations. We discuss these groups separately.

A. Low concentrations, $x < 0.15$

This group of alloys is in good agreement with the RKKY model. The plot shown in Fig. 2 of the Curie-Weiss temperature against concentration is indeed linear. In this graph the value of Θ have been normalized to a carrier density of 1×10^{21}/cm^3. This is done by noting that for the range of carriers in the present alloys, Θ varies approximately with k_f,[18] i.e., as $n^{1/3}$, which is a very small correction. Once this correction is made we have

$$\frac{d\Theta}{dx} = 4.0 \pm 0.3\ ^\circ\text{K/at.\% MnTe}\ .$$

This value is very slightly lower than our previously reported figure[4] which had not been corrected for carrier density. We have also calculated the high-temperature value of the spin from the Curie constant C, using the microprobe concentrations and a g value of 2.0.[19] These spin values are given in the columns headed S_{eff} in Table II. The greatest uncertainty in the determination of the spin values is the absolute calibration of the magnetometer. In particular, the relative position of short samples inside the reference coil can introduce variations up to 10% or 15% in the output signal. Consequently, the maximum overall error in S_{eff} is 10% and to within this accuracy all the low-concentration alloys exhibit a Mn spin of $S=\frac{5}{2}$. The well-defined Curie-Weiss behavior with a $S=\frac{5}{2}$ leads us to the conclusion that at these lower concentrations, Mn supports a *localized* moment in the GeTe host.

Turning to the spin dynamics we see that, as mentioned in Sec. III, the temperature dependence of the magnetization well below T_C obeys Eq. (14) for specimens with $x = 0.05$, 0.10, and 0.15. Figure 8 shows a plot of the coefficient A against $x^{-3/2}$ which is linear as predicted. Taking the slope of this plot and the value of $d\Theta/dx$ above allows us to determine J_{sd} and J_2. From this we find

$$J_{s\text{-}d} = 0.90 \pm 0.05\ \text{eV}\ ,$$

while the Curie temperature for the MnTe becomes

$$\Theta_{MnTe} = -(770 \pm 100)\ ^\circ\text{K}\ .$$

The value of J_{sd} is in remarkable agreement with the figure of 0.8 ± 0.08 eV determined *independently* from transport properties.[5] Also the value of Θ_{MnTe} is quite close to the value of $-585\ ^\circ$K reported for pure MnTe by Komatsubara *et al.*[20] The values of J_{sd} and J_2 permit us to determine the actual spin-wave spectrum of the alloys and this is shown in Fig. 9. We note that $\epsilon(k) \propto k^2$ for $k < 0.3k_F$.

Furthermore, Eqs. (11) and (12) predict that $T_C/\Theta \simeq 0.8$. Reference to Table II shows that in fact when T_C was determined, T_C/Θ falls in the range 0.7 ± 0.2. Since T_C is very sensitive to inhomogeneities, the agreement here is quite satisfactory.

The only feature of these alloys not covered by the simple RKKY theory is the persistence of a

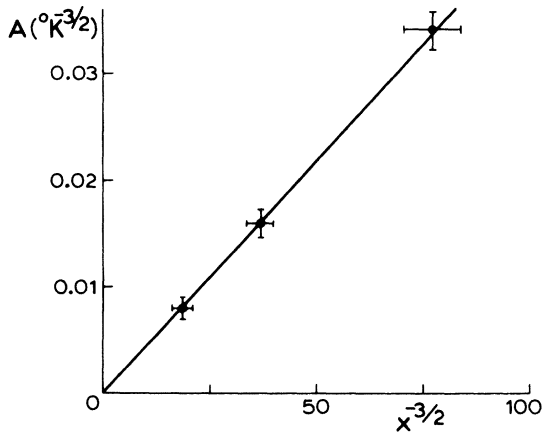

FIG. 8. Spin-wave demagnetization coefficient A as a function of $x^{-3/2}$ for the $x = 0.05$, 0.10, and 0.15 alloys.

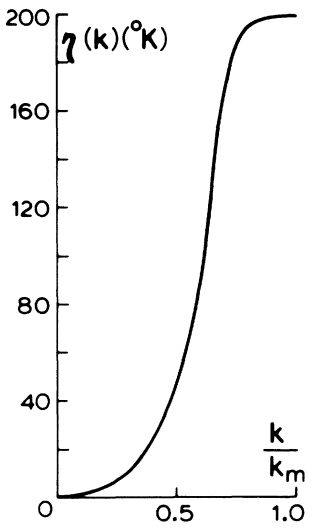

FIG. 9. Spin-wave spectrum as calculated from Eq. (13) using parameters in the text.

finite high-field susceptibility χ_{hf} up to even the highest fields. With this observation it is not surprising then that the magnetic moments extrapolated to zero field are consistently less than expected for a saturated spin-$\frac{5}{2}$ ferromagnet. Two possible effects may contribute to the magnetic hardness of these alloys. First, the microprobe scanning of the samples revealed only a 10% composition fluctuation. However, the beam size in this probe averages over regions at least a micron in diameter, whereas the electron mean free path λ, as estimated from the resistivity, [5] is only 100 Å, some two orders of magnitude smaller. Significant homogeneities in the solute distribution on the scale of 10λ would not be detected in the microprobe scan, but would manifest themselves as composition fluctuations in the magnetic data. The second possible explanation for the magnetic "hardness" arises from neglect of the polarization of the free carriers. This point is discussed below and we note here only that this polarization can be large enough to account for χ_{hf} particulary for the lower-concentration alloys.

B. High concentrations, $x > 0.20$

This group of alloys is not described by the RKKY theory at all. First, the paramagnetic Curie-Weiss temperature deviates from the linear prediction of Eq. (12). The Curie constant for highest-concentration alloys is anomalously low, corresponding in some cases to spin values of less than 2. Furthermore, the Curie plot of $1/\chi$ against T shows considerable curvature even well above T_C. The transition temperature itself is consistently *larger* than Θ in direct contradiction to theory. But the most spectacular behavior is exhibited by the temperature dependence of the magnetization below T_C, as discussed in Sec. III. A *field-independent* $T^{3/2}$ law for the 20-at.% alloys becoming a T^2 law for the 20 and 50-at.% alloys cannot be explained at all on simple spin-wave theory. The most obvious explanation of anomalous behavior is inhomogeneities in Mn distribution. This would certainly account for the curvature of the Curie plot and the high value of T_C. However, it seems most improbable that it could explain the power laws above, which are obeyed very closely and over a wide range of temperature. This suggests that the power laws are an inherent property of the alloys and *not* a reflexion of metallurgical inhomogeneities. The existence of the T^2 power law might be construed as meaning the manganese d levels are forming a band and the demagnetization is caused by Stoner excitations. [21] However, since the d levels in pure MnTe are not believed to form a band it seems unlikely they would do so here where the distance between Mn ions is so much greater.

It seems more convincing, therefore, that the main cause of the divergence between experiment and theory lies in the latter's failure to include the effect of polarization of the free carriers. The low Fermi energy (~ $\frac{1}{2}$ eV) and the high value of J_{sd} (~ 1 eV) results in a very strong coupling between the Mn spins and the free carriers. Indeed, one can estimate that, at $T = 0$, the free carriers are entirely polarized for $x > 0.2$. This polarization significantly affects the RKKY coupling, making it temperature dependent. Moreover, if fully polarized, the bulk magnetization of the carriers is of the same order of magnitude as that of the manganese near $x = 0.1$ and remains significant to all concentrations. Thus, neglect of this effect is anything but trivial, especially in samples of higher concentration where the polarization is larger. At present we are not aware of any theory incorporating these features and hope to return to it at a future time.

VI. CONCLUSIONS

We have carried through a detailed study of the magnetization of a series of $(GeTe)_{1-x}$ $(MnTe)_x$ alloys over the range $0 < x < 0.5$. All the alloys were found to be *ferromagnetic* even though MnTe is itself antiferromagnetic. At low concentrations, ($x < 0.15$) the results are summarized by the distinctive feature that all the experimental magnetic energies, Θ, T_C, and the spin-wave dispersion coefficients are linear in the concentration. This behavior is very well explained by a simple RKKY model with and s-d exchange constant J_{sd}, in excellent agreement with our previously reported independent determination from transport properties. Such distinct RKKY character is usually not ob-

served for these large concentrations of $3d$ ions in metals, but is manifest in the GeTe host because of the relatively low free-carrier density of this system.

For the higher concentrations, the alloys exhibit properties which deviate strikingly from those at lower concentrations, but which nevertheless appear to be intrinsic to the alloys. The Curie-Weiss temperature is no longer linear in the concentration and the simple spin-wave demagnetization is completely lost. These results disagree with the simple RKKY model, but at the same time they underscore the need for a comprehensive treatment of the RKKY interaction including such effects as conduction-electron polarization.

We believe that a clear understanding of these anomalies calls for a wider range of experimental information and have begun an investigation of several related alloy systems such as those with SnTe as host. We hope that this approach will distinguish the features of general significance from those peculiar to a given system.

ACKNOWLEDGMENTS

The authors wish to thank L. Larson of the Department of Metallurgy, McGill University, for carrying out the microprobe analysis. This research was supported by the National Research Council of Canada under Grant No. A5948.

*Present Address: Department of Physics, University of Alberta, Edmonton, Alberta, Canada.

[1]W. D. Johnston and D. E. Sestrich, J. Inorg. Nucl. Chem. 19, 229 (1961).

[2]M. Rodot, J. Lewis, H. Rodot, G. Villers, J. Cohen, and P. Mollard, J. Phys. Soc. Jap. Suppl. 21, 627 (1966).

[3]N. Kunitomi, Y. Hamaguchi, and S. Anzai, J. Phys. 25, 568 (1964).

[4]R. W. Cochrane and J. O. Ström-Olsen, in *Proceedings of the Thirteenth International Conference on Low Temperature Physics, Boulder, Colo.*, 1972, edited by R. H. Kropschot and K. P. Timmerhaus (University of Colorado Press, Boulder, Colo., 1973).

[5]R. W. Cochrane, F. T. Hedgcock, and J. O. Ström-Olsen, Phys. Rev. B 8, 4262 (1973).

[6]N. F. Olivera, Jr. and S. Foner, Rev. Sci. Instrum. 43, 37 (1972).

[7]W. N. R. Stevens, J. Phys. E 4, 850 (1971); J. Phys. E 4, 853 (1971).

[8]M. Springford, J. R. Stockton, and W. R. Wampler, J. Phys. E 4, 1036 (1971).

[9]K. P. Belov and A. N. Goryaga, Fiz. Met. Metalloved. 2, 3 (1956).

[10]M. A. Ruderman and C. Kittel, Phys. Rev. 96, 99 (1954); T. Kasuya, Prog. Theoret. Phys. 16, 45 (1956); K. Yosida, Phys. Rev. 106, 893 (1957).

[11]For reviews see B. R. Cooper, Solid State Phys. 21, 393 (1968); T. Kasuya, in *Magnetism*, edited by G. T. Rado and H. Suhl (Academic, New York, 1966), Vol. 2 B, p. 215.

[12]T. Arai and M. Parinello, Phys. Rev. Lett. 27, 1226 (1971).

[13]L. C. Bartel, Phys. Rev. B 7, 3153 (1973).

[14]R. Tahir Kheli and D. ter Haar, Phys. Rev. 127, 88 (1962).

[15]D. N. Zubarev, Usp. Fiz. Nauk. 71, 71 (1960) [Sov. Phys.-Usp. 3, 320 (1960)].

[16]H. B. Callen, Phys. Rev. 130, 890 (1963).

[17]B. E. Argyle, S. H. Charap, and E. W. Pugh, Phys. Rev. 132, 2051 (1963).

[18]To be precise, only the long-range part of the interaction varies as k_F since the AFM J_2 is a direct nearest-neighbor coupling. However, as the former is the dominant contribution the $n^{1/3}$ variation holds approximately.

[19]F. T. Hedgcock, J. Lass, and T. W. Raudorf, J. Phys. 1, C506 (1971); and also our own unpublished ESR data.

[20]T. Komatsubara, M. Murakami, and E. Hirahara, J. Phys. Soc. Jap. 18, 356 (1963).

[21]See, for example, E. D. Thompson, E. P. Wohlfarth, and A. C. Bryan, Proc. Phys. Soc. Lond. 83, 59 (1964).